Article ID: 1671-3664(2003)02-0281-07

Anti-plane deformations around arbitrary-shaped canyons on a wedge-shape half-space: moment method solutions

Nazaret Dermendjian[1†], Vincent W. Lee[2‡] and Jianwen Liang (梁建文)[3§]

1. *Department of Civil Engineering & Applied Mechanics, California State University, Northridge, California 91330-8347, USA*
2. *Department of Civil & Environmental Engineering, University of Southern California, Los Angeles, California, 90089-2531, USA*
3. *School of Civil Engineering, Tianjin University, Tianjin 300072, China.*

Abstract: The wave propagation behavior in an elastic wedge-shaped medium with an arbitrary shaped cylindrical canyon at its vertex has been studied. Numerical computation of the wave displacement field is carried out on and near the canyon surfaces using weighted-residuals (moment method). The wave displacement fields are computed by the residual method for the cases of elliptic, circular, rounded-rectangular and flat-elliptic canyons. The analysis demonstrates that the resulting surface displacement depends, as in similar previous analyses, on several factors including, but not limited, to the angle of the wedge, the geometry of the vertex, the frequencies of the incident waves, the angles of incidence, and the material properties of the media. The analysis provides intriguing results that help to explain geophysical observations regarding the amplification of seismic energy as a function of site conditions.

Keywords: weighted-residual; moment method; wedge half-space; arbitrary-shaped: cicular, elliptic, rectangular canyons

1 Introduction

The research presented in this paper involves the study of plane SH-waves propagating through a wedge-shaped media. In particular, the geometry of the media ranges from a flat elastic half-space (where the wedge angle is 180°), through the sloping wedge-space with edge angles ($\nu\pi$, $1/2 \le \nu \le 1$) ranging between 180°and 90° from a half space ($\nu = 1$) to a quarter-space ($\nu = 1/2$). Furthermore, an arbitrary shape canyon exists at the vertex of the wedge. Figure 1 illustrates the geometry of a sloping wedge-space for the case of incident plane SH-waves.

Even though the treatment of the problem is somewhat mathematical, it is believed that the consideration of such a problem has practical ramifications, as many homes and other structures have been built on ridges and cliffs overlooking valleys and the ocean. The topography of these ridges can be reasonably characterized in two-dimensions as a wedge-space..

The problem of the two-dimensional scattering and diffraction of plane elastic SH (shear horizontal, anti-plane) waves by a surface canyon in an elastic half-space has been studied by many researchers in earthquake engineering and strong motion seismology, Trifunac (1973) first solved such two-dimensional SH scattering diffraction of plane SH waves by a semi-circular canyon in a flat elastic half space. Wong and Trifunac (1974a,b) solved the same problem for semi-elliptical canyons and alluvial valleys. Cao and Lee (1989, 1990), Lee and Cao (1989) extended Trifunac's (1973) results to cases involving shallow circular canyons respectively for incident SH, P and SV waves. Lee (1982, 1984, 1988, 1990) further studied diffraction problems for hemispherical canyons, valleys and parabolic canyons. The common feature of the above papers is that all of the canyons are either circular, elliptic or parabolic in shape. In other words, they are all of regular shapes. This allows all of the above analyses to give closed-form analytic series as solutions to the problems. Good references for elastic wave propagation problems are found in texts by Mow and Pao (1971), Achenbach (1973), and Graff (1991).

For canyons with irregular shapes, field computations will have to be carried out by numerical approximations (Wong *et al*, 1997, Sanchez-Sesma and Rosenbleuth, 1979). Some popular methods in the analyses of wave diffractions are the finite difference method (FDM), the finite element method (FEM), and the boundary element method (BEM).

As pointed out in Lee and Wu (1994a,b), with FDM or FEM, material inhomogeneouity and irregular geometry can be easily modeled. However dealing with semi-infinite or infinite domains, which are usually associated with the problem of wave scattering and diffraction, some approximations have to be introduced. The most

Correspondence to: Nazaret Dermendjian, Department of Civil Engineering & Applied Mechanics, California State University, Northridge, California 91330-8347, USA.
Fax: 1-818-6775810
E-mail: nazaret.dermendjian@csun.edu
†Assistant Professor; ‡Professor; §Professor

Received date: 2003-07-15; **Accepted date:** 2003-11-04

general method is to simply truncate the infinite or semi-infinite domains into finite ones. In this way, artificial boundaries will have to be created and they will prevent the true propagation of the waves, thus introducing errors. Another difficulty is that FDM and FEM may be easily overwhelmed by the large physical dimensions or the fine details of the requirement, so for seismic wave analysis in a semi-infinite domain, they would numerically become a large-sized problem. The BEM, on the other hand, does not have these disadvantages; it only needs to perform integration along the boundaries and model the infinite domain very well. Theoretically, it is very suitable for the problems with infinite or semi-infinite geometries. It, however, encounters the difficulty in dealing with the Green's function singularities in the path of numerical integration.

With this difficulty in mind, Lee and Wu (1994a,b) chose instead the so-called "weighted residual" or "moment" method to solve these diffraction problems involving arbitrary shaped canyons. This method is used abundantly both in the fields involving electromagnetic and acoustic waves. See Harrington (1967) for a full historical development and references of this method.

In the weighted residual method used in this study, like the BEM, it only needs to be integrated along the original boundaries. Thus the size of the equations is greatly reduced, when compared with that of the FDM and FEM, and it imposes no artificial boundaries at all. It also does not involve the Green's function, thus avoiding the difficulty of singularities that the other methods encounter. Compared with the method of using the simple full space Green's function (Chang and Wong, 1990), the results of the weighted residual method are much better for relatively deep canyons. Beside all of these advantages, it is also simple to formulate. Therefore the weighted residual proposed here is very suitable for wave scattering and diffraction problems.

Lee and Sherif (1996) presented such a diffraction problem involving a circular canyon at the vertex of the wedge space. The solution is expressible in simple analytic closed form involving Hankel functions with the corresponding cosine terms.

The analysis indicates that SH-waves travelling through a particular wedge geometry result in displacement fields that depend on the angle of incidence, the frequency of the incident wave, the geometry of the vertex and the material properties of the media.

2 SH wave propagation in an elastic wedge

The two-dimensional model of the problem is shown in Fig.1. It represents the wedge-shaped space with angle $\nu\pi$, where $1/2<\nu<1$. An arbitrary-shaped canyon is situated on the vertex of the wedge space. Both the rectangular (x,y) and cylindrical (r,θ) coordinate systems are defined on the model. The wedge-shaped space is assumed to be elastic, isotropic and homogeneous, with the material properties given by Lame constants λ and μ and by the mass density ρ, from which the shear wave speed, $C_\beta = (\mu/\rho)^{1/2}$ is derived.

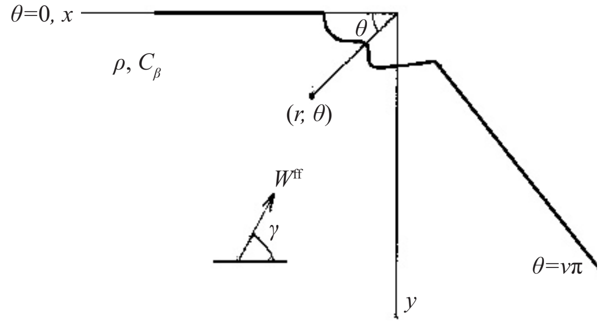

Fig. 1 Arbitrary shaped canyon – the model

For incident plane SH waves with incident angle γ with respect to the horizontal, the free-field equation is (Sanchez-Sesma, 1985; Lee and Sherif, 1996)

$$W^{ff} = \frac{2}{\nu}\sum_{n=0}^{\infty}\varepsilon_n e^{\frac{-in\pi}{2\nu}} J_{\frac{n}{\nu}}(kr)\cos(\frac{n\gamma}{\nu})\cos(\frac{n\theta}{\nu}) \tag{1}$$

where $\varepsilon_0 = 1$, and $\varepsilon_n = 2$ for $n > 0$. The presence of the arbitrary-shaped canyon will result in the scattered waves which are given by the equation (Lee and Sherrif, 1996)

$$W^{s} = \sum_{n=0}^{\infty} A_n H^{(1)}_{\frac{n}{\nu}}(kr)\cos(\frac{n\theta}{\nu}) \tag{2}$$

Both the free-field and scattered waves W^{ff} and W^{s} satisfy the free field boundary condition:

$$\tau_{z\theta} = \frac{\mu}{r}\frac{\partial}{\partial\theta}W^{s} = 0, \quad \text{at } \theta = 0, \nu\pi \tag{3}$$

At C, the surface of the canyon, the zero-stress boundary condition is

$$\tau_{nz} = \mu\frac{\partial W}{\partial n} = \mu(\frac{\partial W}{\partial r}n_r + \frac{1}{r}\frac{\partial W}{\partial\theta}n_\theta) = 0 \tag{4}$$

where $\boldsymbol{n}$ is the normal at every point of the cavity surface, such that $\boldsymbol{n} = n_r\boldsymbol{e}_r + n_\theta\boldsymbol{e}_\theta$. Eq. (4) can not be satisfied analytically along C, the surface of the arbitrary shaped canyon.

3 The weighted residual (moment) method

The weighted residual method, also known as the moment method, is used as a numerical method for the evaluation of the displacement field (Lee and Wu, 1994a,b; Lee and Manoogian, 1995). Weight functions are selected along the surface of the canyon C, such that $W_m = W_m(\theta)$ for $m = 0,1,2,3,\ldots$ and along C

$$\int_0^{\nu\pi}\tau^{s}_{nz}W_m\,\mathrm{d}\theta = -\int_0^{\nu\pi}\tau^{ff}_{nz}W_m\,\mathrm{d}\theta \tag{5}$$

where the stress due to the scattered waves is given by

$$\tau_{nz}^{s} = \tau_{nz}(r(\theta),\theta) = \mu\left(\frac{\partial W^{s}}{\partial r}n_{r} + \frac{1}{r}\frac{\partial W^{s}}{\partial \theta}n_{\theta}\right) = L(W^{s}) =$$

$$L\left(\sum_{n=0}^{\infty} A_{n} \mathrm{H}^{(1)}_{\frac{n}{\nu}}(kr(\theta))\cos\frac{n\theta}{\nu}\right) = \sum_{n=0}^{\infty} A_{n} L(f_{n})$$

$$\tau_{nz}^{\mathrm{ff}} = \tau_{nz}(r(\theta),\theta) = -g(\theta) \tag{6}$$

as the stresses due to the input free-field waves. Eq. (5) becomes with

$$\langle W_{m}, L(f_{n})\rangle = \int_{0}^{\nu\pi} W_{m}(\theta) L(f_{n}) \mathrm{d}\theta$$

$$\sum_{n=0}^{\infty} \langle W_{m}, L(f_{n})\rangle A_{n} = \langle W_{m}, g\rangle = g_{m} \tag{7}$$

$$\boldsymbol{C}\,\boldsymbol{A} = \boldsymbol{g}$$

and thus the coefficients $\boldsymbol{A}$ can be calculated. A good choice for the weight function is

$$W_{m}(\theta) = \cos\frac{m\theta}{\nu} \tag{8}$$

4. Case of Semi-cirlar canyon

The case of the semi circular (Fig.2) in an elastic wedge-shaped half space has an exact closed form solution for an incident plane SH wave (Lee and Sherif, 1996). The solution of the weighted-residual method obtained above can thus be compared with the exact solution.

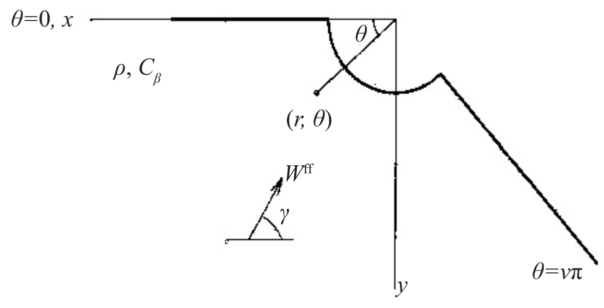

Fig. 2 Circular canyon

The free-field motion given by Eq. (1) and the scattered waves given by Eq. (2) are repeated here with the value of r given as a, the radius of the semi circular canyon.

$$W^{\mathrm{ff}} = \frac{2}{\nu}\sum_{n=0}^{\infty} \varepsilon_{n} \mathrm{e}^{\frac{-\mathrm{i}n\pi}{2\nu}} \mathrm{J}_{n/\nu}(ka)\cos\left(\frac{n\gamma}{\nu}\right)\cos\left(\frac{n\theta}{\nu}\right) \tag{9}$$

$$W^{s} = \sum_{n=0}^{\infty} A_{n} \mathrm{H}^{(1)}_{n/\nu}(ka)\cos\left(\frac{n\theta}{\nu}\right) \tag{10}$$

At the surface of the circular canyon, the boundary conditions expressed by Eq. (3), are reduced to Eq. (11) below

$$\tau_{nz} = \mu\frac{\partial W}{\partial r} = \mu\frac{\partial}{\partial r}\left(W^{\mathrm{ff}} + W^{s}\right)\Big|_{r=a} = 0 \tag{11}$$

Substituting Eqs. (9) and (10) in Eq. (11), the coefficients A_n are thus calculated by

$$A_{n} = -\frac{2}{\nu}\varepsilon_{n} \mathrm{e}^{\frac{-\mathrm{i}n\pi}{2\nu}} \frac{\mathrm{J}'_{n/\nu}(ka)}{\mathrm{H}^{(1)'}_{n/\nu}(ka)}\cos\left(\frac{n\gamma}{\nu}\right) \tag{12}$$

The scattered waves are thus presented by Eq.(13) below,

$$W^{s} = -\sum_{n=0}^{\infty}\frac{2}{\nu}\varepsilon_{n} \mathrm{e}^{\frac{-\mathrm{i}n\pi}{2\nu}} \frac{\mathrm{J}'_{n/\nu}(ka)}{\mathrm{H}^{(1)'}_{n/\nu}(ka)} \mathrm{H}^{(1)}_{n/\nu}(ka)\cos\left(\frac{n\theta}{\nu}\right)\cos\left(\frac{n\gamma}{\nu}\right) \tag{13}$$

It is worth comparing this exact closed form solution with that obtained from the weighted-residual method presented earlier. Thus, starting with Eq. (2) and utilizing Eq. (11), with the stresses defined in Eqs.(14) and (15) below,

$$\tau_{nz}^{\mathrm{ff}} = \sum_{n=0}^{\infty} \varepsilon_{n} \mathrm{e}^{\frac{-\mathrm{i}n\pi}{2\nu}} \mathrm{J}'_{n/\nu}(ka)\cos\left(\frac{n\theta}{\nu}\right)\cos\left(\frac{n\gamma}{\nu}\right) \tag{14}$$

$$\tau_{nz}^{s} = \sum_{n=0}^{\infty} A_{n} \mathrm{H}^{(1)'}_{n/\nu}(ka)\cos\left(\frac{n\theta}{\nu}\right) \tag{15}$$

and using a weight function $w_m = \cos(m\theta/\nu)$, m=0,1,2,…, the following inner products are evaluated:

$$\langle w_{m}, \tau_{nz}^{s}\rangle = A_{n} \mathrm{H}^{(1)'}_{n/\nu}(ka)\int_{0}^{\nu\pi}\cos\left(\frac{m\theta}{\nu}\right)\cos\left(\frac{n\theta}{\nu}\right)\mathrm{d}\theta \tag{16}$$

Utilizing the orthogonality of the cosine functions, i.e.

$$\int_{0}^{\nu\pi}\cos\left(\frac{m\theta}{\nu}\right)\cos\left(\frac{n\theta}{\nu}\right)\mathrm{d}\theta = \begin{cases}\frac{\nu\pi}{2}, & m = n \neq 0\\ 0, & m \neq n\end{cases} \tag{17}$$

When $m = n = 0$, the above integral equals $\nu\pi$. The inner product for the plane SH waves is represented by

$$\langle w_{m}, \tau_{nz}^{\mathrm{ff}}\rangle = \frac{2}{\nu}\varepsilon_{n} \mathrm{e}^{\frac{-\mathrm{i}n\pi}{2\nu}} \mathrm{J}'_{n/\nu}(ka)\cos\left(\frac{n\gamma}{\nu}\right)\cdot$$

$$\int_{0}^{\nu\pi}\cos\left(\frac{m\theta}{\nu}\right)\cos\left(\frac{n\theta}{\nu}\right)\mathrm{d}\theta \tag{18}$$

with the orthogonality of the cosine functions as before, and substituting Eqs. (16) and (18) in Eq. (11), it is observed that the matrix in Eq. (7) is diagonal, and thus the coefficients A_n's are evaluated as,

$$A_n H^{(1)'}_{n/\nu}(ka)\cdot\frac{\nu\pi}{2}+\frac{2}{\nu}\varepsilon_n e^{\frac{-in\pi}{2\nu}} J'_{n/\nu}(ka)\cos\left(\frac{n\gamma}{\nu}\right)\cdot\frac{\nu\pi}{2}=0 \tag{19}$$

and thus

$$A_n=-\frac{2}{\nu}\varepsilon_n e^{\frac{-in\pi}{2\nu}}\frac{J'_{n/\nu}(ka)}{H^{(1)'}_{n/\nu}(ka)}\cos\left(\frac{n\gamma}{\nu}\right) \tag{20}$$

which is identical to Eq. (12), the analytical evaluation of A_n. In other words, the appropriate choice of the weight functions results in the exact closed form solution for the case of the semi-circular canyon.

5 Displacement amplitudes

The above analyses for arbitrary-shaped canyons are applied for the following cases of canyons described below.

5.1 Elliptic canyon

The displacement amplitudes for elliptic canyons are evaluated for the shape defined by

$$\left(\frac{x}{a}\right)^2+\left(\frac{y}{b}\right)^2=1 \tag{21}$$

for ratios of b/a of 0.75 to 1.25. When the b/a ratio is 1, the shape is circular and is compared with the solution of Lee and Sherif, 1996. The results of the circular canyon on half space, where the wedge angle $\nu\pi$ = 180°, are compared with existing analytic solutions presented by Trifunac, 1973. The results of the elliptical canyon on half space, where the wedge angle $\nu\pi$ = 180°, are compared with the existing analytic solutions presented by Wong and Trifunac (1974).

The wedge angles studied are 90°, 120°, 150° and 180°. Fig.3 represents the displacement amplitudes for elliptic canyons with wedge angles of $\nu\pi$ = 90° and varying angles of incidence. The graphs are three

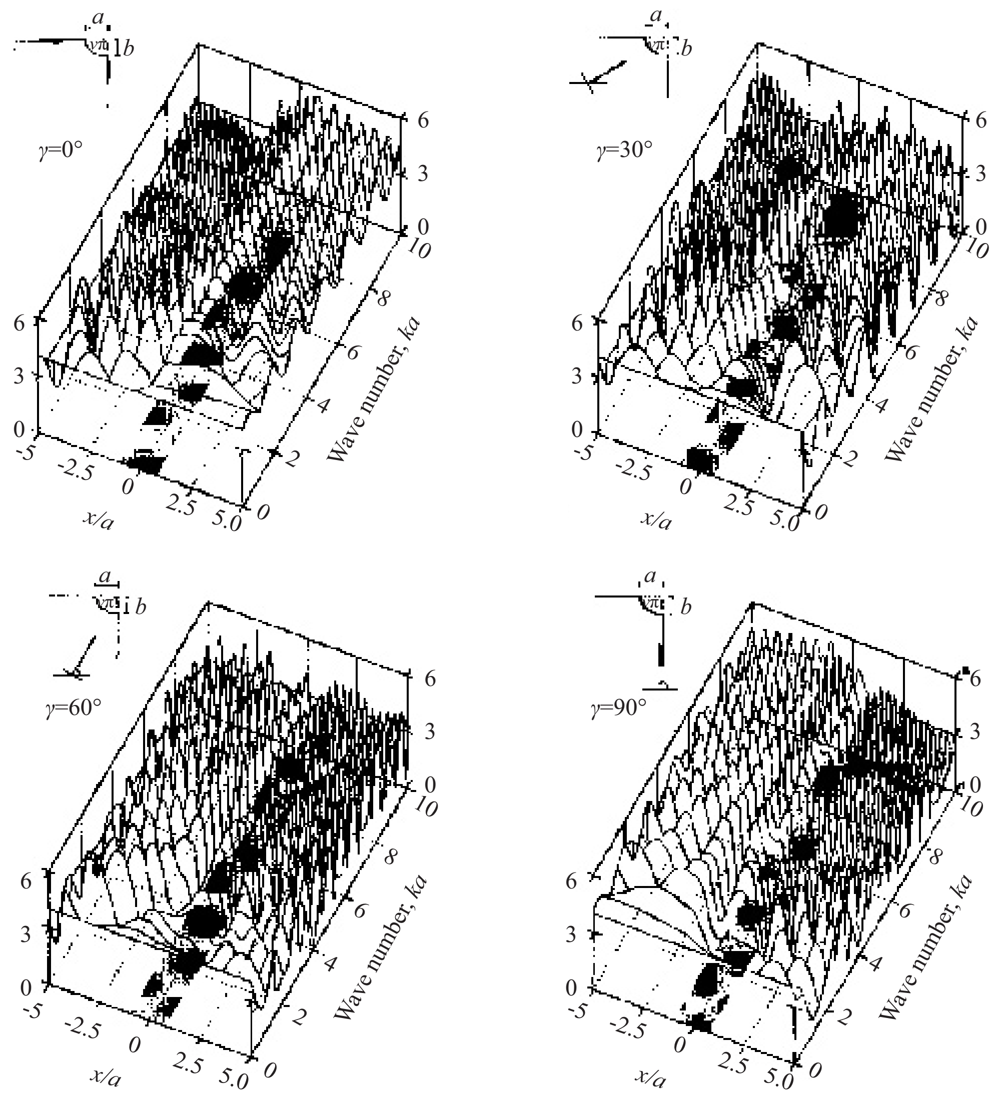

Fig. 3 Anti-plane surface displacement amplitudes (elliptic canyon on wedge space, wedge angle $\nu\pi$ = 90°, b/a = 0.75)

plots representing the displacement amplitudes for incident plane SH waves with amplitude of 1.

For all graphs, the displacement amplitudes are plotted versus the dimensionless distance x/a labeled to range between values of −5 and 5, and the frequency (wave number) ka, ranging between values of 0 and 10. Note that these distances are not the coordinates on the axis used, but just for visual convenience. The labels $x/a < -1$ thus correspond to points on the horizontal surface of the wedge-space to the left of the canyon. Distances $-1 < x/a < b/a$ (the shaded part in the figure) correspond to points on the surface of the canyon, and distances $x/a > b/a$ correspond to points on the inclined surface of the wedge-space to the right of the canyon. The origin is taken as shown in Fig.1, at the point of intersection of the horizontal and the inclined surfaces of the wedge with the positive x-axis to the left on the origin and the positive y-axis vertically downward.

In addition, for all graphs, the stress-free boundary condition on the horizontal and the inclined surfaces of the wedge-space, i.e. where $x/a < -1$ and $x/a > b/a$, are automatically satisfied and thus no integration is carried out at those surfaces. Integration is carried out on the points that are on the surface on the canyon using the (moment) method of weighted-residuals.

5.2 Elliptic-flat beyond 90° canyon

The displacement amplitudes of elliptic canyons with flat surface beyond 90° are evaluated for the shape defined by Eq. (9) earlier for the elliptic part of the canyon and by a flat surface for the surface beyond the 90°. The analyses are again for b/a ratios of 0.75 to 1.25. The wedge angles studied are again 90°, 120°, 150° and 180°. Fig. 4 shows the displacement amplitudes for elliptic canyons with flat surface beyond 90° with wedge angle of 120° and four angles of incidence.

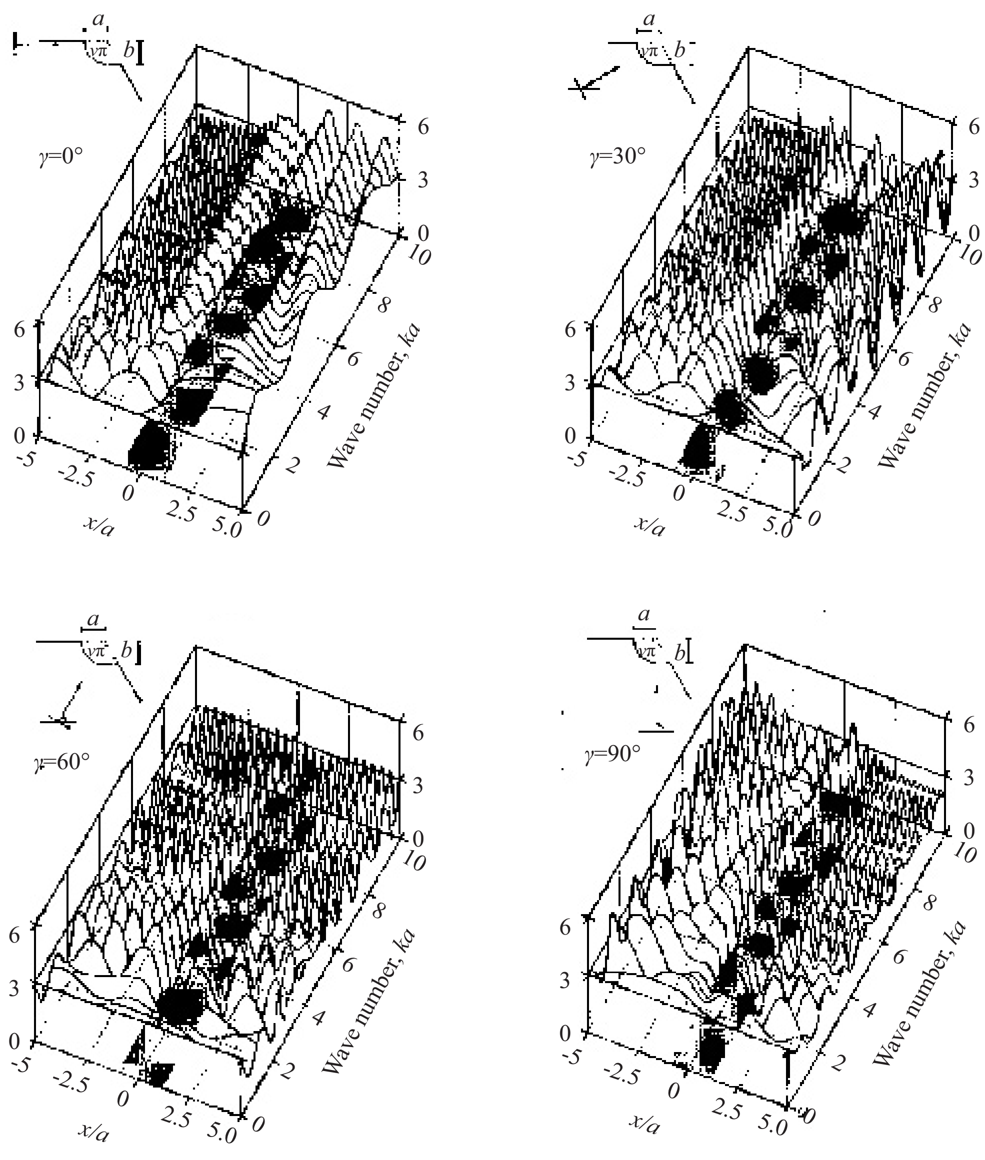

Fig. 4 Anti-plane surface displacement amplitudes (flat circular canyon on wedge space, wedge angle: $\upsilon\pi$ = 120°, b/a = 1.00)

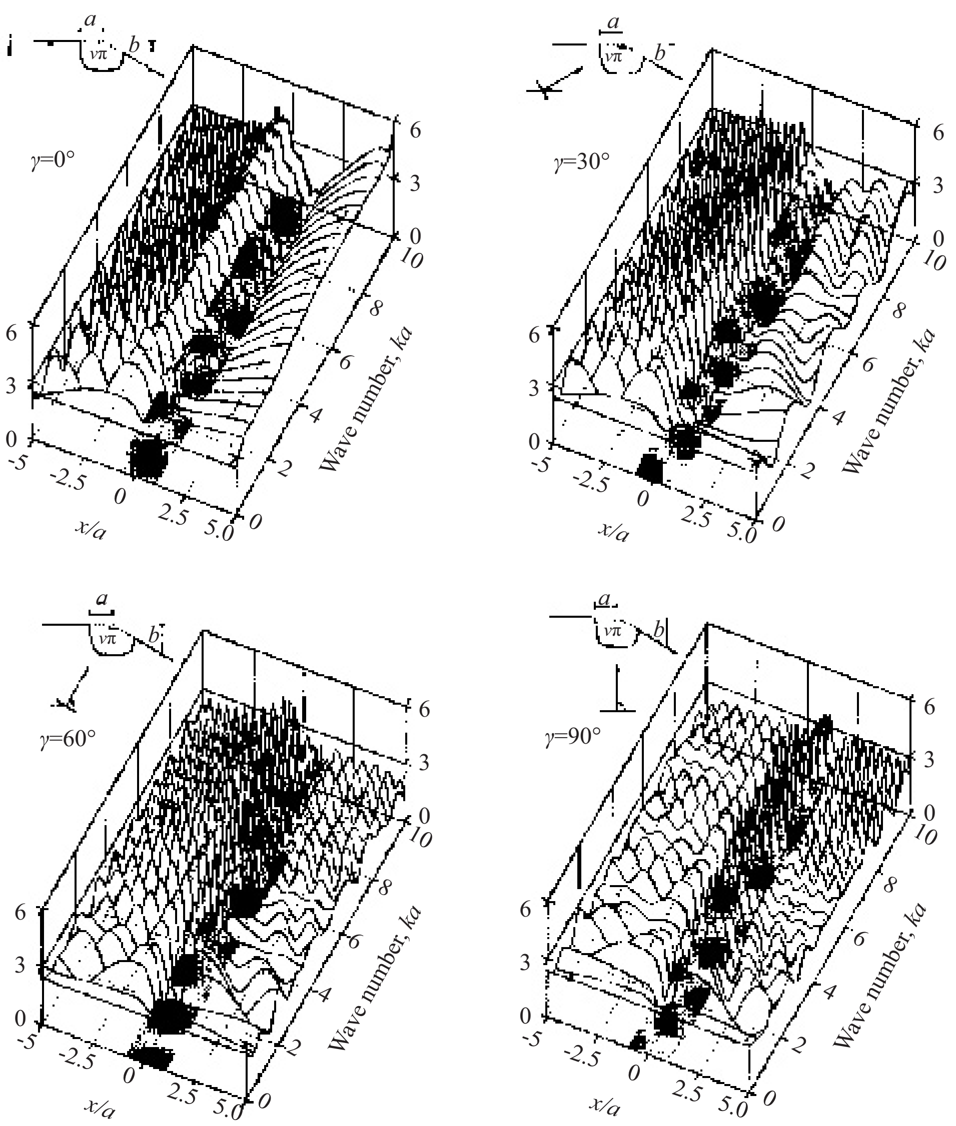

Fig. 5 Anti-plane surface displacement amplitudes ("rounded" rectangular canyon on wedge space, wedge angle $\upsilon\pi$ = 150°, b/a = 1.25)

5.3 Rounded-rectangular canyon

The displacement amplitudes for rounded-rectangular canyons are evaluated for the shape defined by

$$\frac{y}{a}=\frac{b}{a}\left\{1-\exp\left[-\alpha\left(1-\frac{1-|x|/a}{\alpha}\right)\right]\right\} \tag{22}$$

where $\alpha > 0$ is a positive integer large enough so that the graph of the function resembles a rectangular shape with "rounded" corner. In this analysis, a value of α = 8 is used. Again, the analyses and calculations are for b/a ratios of 0.75 to 1.25. The wedge angles studied are 90°, 120°, 150° and 180°. Fig.5 shows the displacement amplitudes for rounded-rectangular canyons with wedge angle of $v\pi$ = 150° and four angles of incidence.

For the weighted-residual method, as many as N = 20 terms are used to achieve convergence at high frequencies. The agreement of the results with existing analytic solutions is good.

6 Conclusions

The displacement amplitudes calculated on or near arbitrary, wedge-shaped canyons show that the response is dependent on all the parameters used in the analysis, including but not limited to the angle of incidence, frequency of the incoming train of the SH waves, the geometry of the canyon and the material properties of the media. A complete set of figures for all four angles of incidence, 0°, 30°, 60° and 90°, and various wedge angles, 90°, 120°, 150° and 180° at dimensionless frequencies up to ka=10 can be found in Dermendjian and Lee (2002). The case of the wedge angle of 180° have results that are in agreement with previous known analytic and numerical solutions (Lee and Cao, 1989; Lee and Wu, 1994a).

The present case of an arbitrary-shaped cylindrical canyon on the vertex of a wedge space is an extension of the same problem in a flat half space. While there are not many practical canyon topographies that will fit the geometry of the canyons studied here, the present paper present a methodology from which more complicated problems can be built on and solved. For example, the same weighted-residual moment method has next been applied to arbitrary-shaped foundations in soil-structure-interaction (SSI) studies on wedge-shaped half-space to be presented in subsequent papers.

References

Achenbach JD (1973), *Wave Propagation in Elastic Solids*, North-Holland Publishing Company.

Cao H and Lee VW (1989), "Scattering of Plane SH Waves by Circular Cylindrical Canyons of Various Depth-to-Width Ratios," *European Journal of Earthquake Engineering*, **2**: 29-37.

Cao H and Lee VW (1990), "Scattering and Diffraction of Plane P Waves by Circular Cylindrical Canyons with Variable Depth-to-Width Ratios," *International Journal of Soil Dynamics and Earthquake Engineering*, **9**(3): 141-150.

Chang WL and Wong HL (1990), "Boundary Integral Equation Method for the Diffraction of Elastic Waves Using Simplified Green's Functions," *PhD Thesis,* Univ. of Southern California, Los Angeles, California.

Dermendjian N and Lee VW (2002), "Soil-Structure Interaction and Diffraction of Anti-plane (SH) Waves Around Topogrphies in a Wedge-Shaped Elastic Half-Space," *PhD Thesis*, Univ. of Southern California, Los Angeles, California.

Graff KF (1991), *Wave Motion in Elastic Solids*, Ohio State University Press.

Harrington RF (1967), Matrix Methods for Field Problems, *Proceedings of the IEEE*, **55**(2).

Lee VW (1982), "A Note on the Scattering of Elastic Plane Waves by a Hemispherical Canyon," *International Journal of Soil Dynamics and Earthquake Engineering*, **1**(3): 122-129.

Lee VW (1984), "Three-Dimensional Diffraction of Plane P, SV and SH Waves by a Hemispherical Alluvial Valley," *International Journal of Soil Dynamics and Earthquake Engineering*, **3**(3): 133-144.

Lee VW (1988), "Three-Dimensional Diffraction of Elastic Waves by a Spherical Cavity in an Elastic Half-Space I: Closed-Form Solutions," *International Journal of Soil Dynamics and Earthquake Engineering*, **7**(3): 149-167.

Lee VW (1990), "On the Scattering of Plane SH Waves By a Semi-Parabolic Cylindrical Canyon in an Elastic Half-Space," *Geophysical Journal*, **100**: 79-86.

Lee VW and Cao H (1989), "Diffraction of SV Waves by Circular Cylindrical Canyons of Various Depths," *ASCE, Engineering Mechanics Division,* **115**(9): 2035-2056.

Lee VW and Manoogian ME (1995), "Surface Motion Above an Arbitrary Shaped Underground Cavity for Incident SH Waves," *European Earthquake Engineering*, **8**(1): 3-11.

Lee VW and Sherif R (1996), "Diffraction around Circular Canyon in Elastic Wedge Space by plane SH-Waves," *Journal of Engineering Mechanics,* ASCE, **122**(6): 539-544.

Lee VW and Wu X (1994a), "Application of the Weighted Residual Method to Diffraction by 2-D Canyons of Arbitrary Shape: I. Incident SH Waves," *Soil Dynamics and Earthquake Engineering* **13**: 355-364.

Lee VW and Wu X (1994b), "Application of the Weighted Residual Method to Diffraction by 2-D Canyons of Arbitrary Shape, Incident P, SV and Rayleigh Waves," *International Journal of Soil Dynamics and Earthquake Engineering*, **13**(5): 365-373.

Mow CC and Pao YH (1971), "The Diffraction of Elastic Waves and Dynamic Stress Concentrations," *RAND Report R-482-PR*, RAND Corporation, Santa Monica.

Sanchez-Sesma FJ (1985), "Diffraction of Elastic SH-Waves in Wedges," *Bulletin of the Seismological Society of America*, **75**(5): 1435-1446.

Sanchez-Sesma FJ and Rosenbleuth E (1979), "Ground Motion at Canyons of Arbitrary Shape under incident SH-Waves," I*nternational Journal of Erathquake Engineering and Structural Dynamics*, **7**: 441-45.

Trifunac MD (1973), "Scattering of Plane SH Waves by a Semi-Cylindrical Canyons," *Journal of Earthquake Engineering and Structural Dynamics*, **1**: 267-281.

Wong HL and Trifunac MD (1974a), "Scattering of Plane SH waves by Semi-Elliptical Canyons," *Journal of Earthquake Engineering and Structural Dynamics,* **3**: 157-169.

Wong HL and Trifunac MD (1974b), "Surface Motion of a Semi-Elliptical Alluvial Valley for Incident Plane Waves," *Bulletin of the Seismological Society of America*, **64**: 1389-140.

Wong HL Trifunac MD and Westermo B (1977), "Effects of Surface and Subsurface Irregularities on the Amplification of Monochromatic Waves," *Bulletin of the Seismological Society of America*, **67**: 353-368.